RESEARCH ARTICLE

A multi-proxy assessment of the impact of environmental instability on Late Holocene (4500-3800 BP) Native American villages of the Georgia coast

Carey J. Garland[1]*, Victor D. Thompson[1], Matthew C. Sanger[2‡], Karen Y. Smith[3‡], Fred T. Andrus[4‡], Nathan R. Lawres[5‡], Katharine G. Napora[6‡], Carol E. Colaninno[7‡], J. Matthew Compton[8‡], Sharyn Jones[9‡], Carla S. Hadden[10‡], Alexander Cherkinsky[10‡], Thomas Maddox[10‡], Yi-Ting Deng[10‡], Isabelle H. Lulewicz[11‡], Lindsey Parsons[1‡]

1 Department of Anthropology, Laboratory of Archaeology, University of Georgia, Athens, Georgia, United States of America, 2 National Museum of the American Indian, Washington, D.C., United States of America, 3 South Carolina Department of Natural Resources, Columbia, South Carolina, United States of America, 4 Department of Geological Sciences, University of Alabama, Tuscaloosa, Alabama, United States of America, 5 Department of Anthropology and Antonio J. Waring Jr. Laboratory of Archaeology, University of West Georgia, Carrollton, Georgia, United States of America, 6 Department of Anthropology, Office of State Archaeology, William S. Webb Museum of Anthropology, University of Kentucky, Lexington, Kentucky, United States of America, 7 Center for STEM Research, Education, and Outreach, Southern Illinois University Edwardsville, Edwardsville, Illinois, United States of America, 8 Department of Sociology and Anthropology, Georgia Southern University, Statesboro, Georgia, United States of America, 9 Department of Anthropology, 217 Landrum Academic Center, Northern Kentucky University, Highland Heights, Kentucky, United States of America, 10 Center for Applied Isotope Studies, University of Georgia, Athens, Georgia, United States of America, 11 Illinois State Archaeological Survey, University of Illinois at Urbana-Champaign, Collinsville, Illinois, United States of America

☯ These authors contributed equally to this work.
‡ These authors also contributed equally to this work.
* carey.garland@uga.edu

Abstract

Circular shell rings along the South Atlantic Coast of North America are the remnants of some of the earliest villages that emerged during the Late Archaic (5000–3000 BP). Many of these villages, however, were abandoned during the Terminal Late Archaic (ca 3800–3000 BP). We combine Bayesian chronological modeling with mollusk shell geochemistry and oyster paleobiology to understand the nature and timing of environmental change associated with the emergence and abandonment of circular shell ring villages on Sapelo Island, Georgia. Our Bayesian models indicate that Native Americans occupied the three Sapelo shell rings at varying times with some generational overlap. By the end of the complex's occupation, only Ring III was occupied before abandonment ca. 3845 BP. Ring III also consists of statistically smaller oysters harvested from less saline estuaries compared to earlier occupations. Integrating shell biochemical and paleobiological data with recent tree ring analyses shows a clear pattern of environmental fluctuations throughout the period in which the rings were occupied. We argue that as the environment became unstable around 4300 BP, aggregation at villages provided a way to effectively manage fisheries that are highly sensitive to environmental change. However, with the eventual collapse of oyster fisheries

and subsequent rebound in environmental conditions ca. post-3800 BP, people dispersed
from shell rings, and shifted to non-marine subsistence economies and other types of settle-
ments. This study provides the most comprehensive evidence for correlations between
large-scale environmental change and societal transformations on the Georgia coast during
the Late Archaic period.

Introduction

The emergence of village life and adaptation to coastal environments are significant transitions
in human history that have occurred at various times and places across the globe. Archaeolo-
gists in southeastern North America, specifically, have long been interested in social, political,
economic, and environmental contexts surrounding the formation and abandonment of early
villages along the South Atlantic Coast during the Late Holocene (5000–3000 BP). Late Holo-
cene (hereafter referred to as the Late Archaic) arcuate and circular shell rings on the Georgia
and South Carolina coasts represent what is left of the earliest village communities that
emerged in this region. Archaeological research on these circular villages, which predate the
adoption of farming, has broadened our understanding of hunter-gatherer economies, the
nature of ceremonialism and early monumentality, cooperation, as well as adaptation and
resilience in the face of environmental instability [1–4]. However, circular shell ring villages of
the South Atlantic coast did not persist across time, and many, especially those of Georgia and
South Carolina, were abandoned towards the end of the Late Archaic. Previous research has
focused on the socio-ecological transformations that occurred during the time in which shell
ring villages were abandoned in the region, yet few researchers have examined the material
record for potential environmental correlations to both the emergence and abandonment of
circular shell ring villages. Further, much of the previous research on this topic tends to
encompass coarse time scales, lacking the granular resolution necessary to understand how
successive generations of people experienced such environmental shifts. Here, we provide a
case study from Sapelo Island, Georgia, to document multiple lines of evidence for types of
environmental shifts experienced by several generations of villagers that lead to societal trans-
formations on the Georgia coast during the Late Archaic.

Circular shell rings along the southeastern Atlantic seaboard of North America emerged
around 4400 cal. BP as marsh ecosystems formed in the context of rising relative sea levels,
which at that time had reached 1.2 m below present (mbp) [5,6]. Environmental shifts, such as
changing temperatures, increased fluctuations in rainfall patterns, and relative sea level
changes (which may have dropped by as much as 2.5 mbp by 3800 cal. BP and 3.5 mbp by
3100 cal. BP), however, are thought to have led to the eventual abandonment and cessation of
shell ring construction in the region [7–9]. Several studies suggest that the abandonment of
shell ring villages corresponded with an environmentally correlated collapse in oyster fisheries
at this time [7,8]. Recent research examines the extent to which the hunter-gatherer communi-
ties of the Georgia coast underwent reorganization in terms of both settlement and economies
to navigate shifting environmental conditions [9,10]. Specifically, Turck and Thompson [9]
argue that hunter-gatherer communities of this region were resilient in the sense that through
cooperation and collective agency these communities were able to negotiate shifting social and
environmental landscapes in the face of environmental change. As environmental shifts
changed resource bases (e.g., reduced productivity of oyster reefs), people reorganized their
social systems, resulting in changing economies, settlement patterns, and spatial layouts of
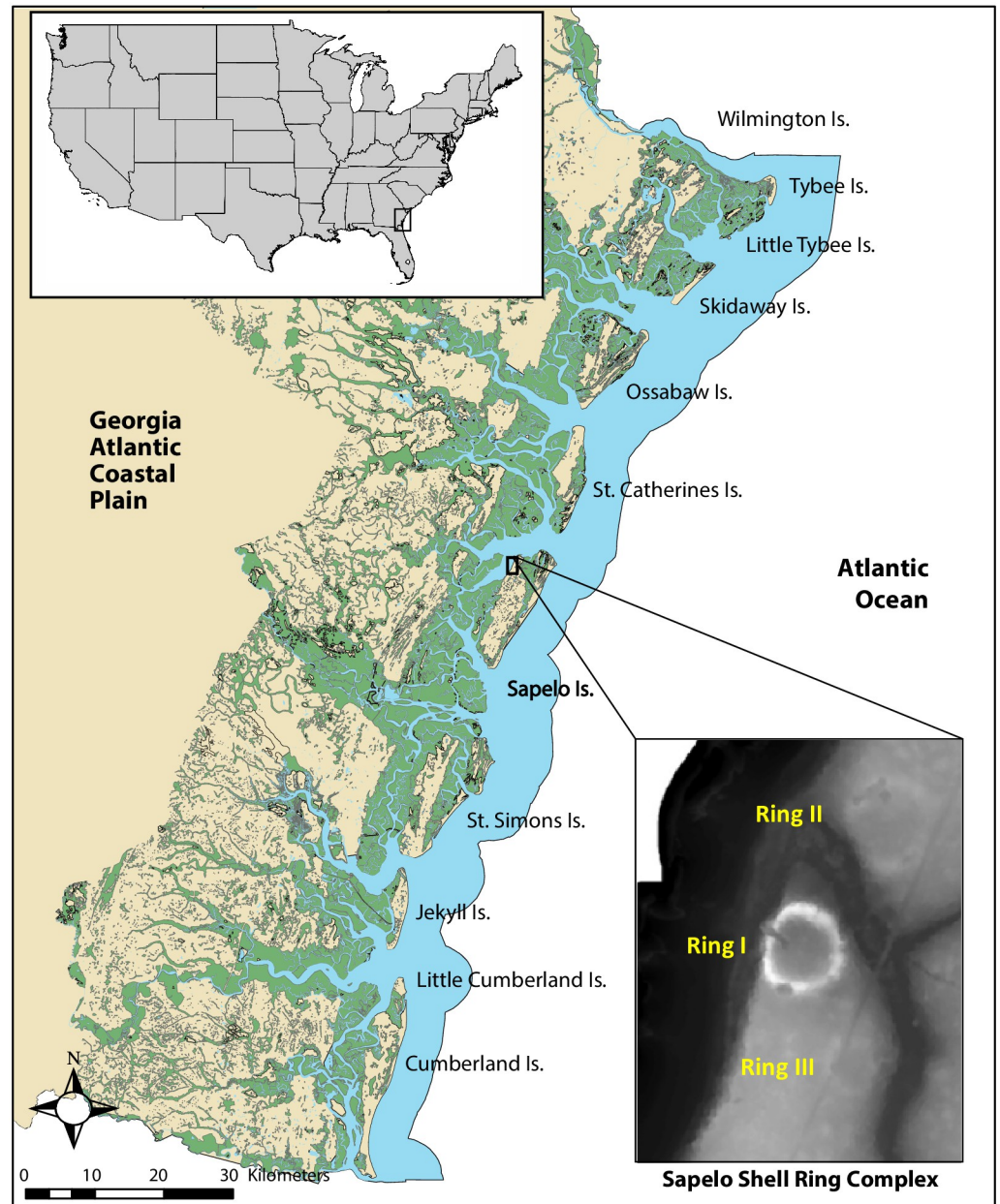
Fig 1. Map of the Georgia coast showing the location of Sapelo Island and shell rings. The map was created by CJG and VDT using ArcGIS Pro and wetland shapefile data from Georgia GIS Clearinghouse (https://data.georgiaspatial.org/index.asp).

https://doi.org/10.1371/journal.pone.0258979.g001

villages (e.g., the shift to non-shell ring sites that evidence a much-reduced reliance on oysters and other shellfish).

Some of the more well-studied Late Archaic shell-rings villages are located on Sapelo Island, Georgia. Sapelo Island, a barrier island located on the Georgia Coast some 80 km south of present-day Savannah, Georgia USA, plays an important role in our understandings of change and continuity in Native American coastal economies, political organization, and settlement patterns in much of the published literature on the subject over the last two decades (Fig 1). More specifically, archaeological and ethnohistorical data from Sapelo Island, and other

barrier islands in the region, suggests that the last 5,000 years of human history on the Georgia coast is characterized by (1) increased population growth, (2) a shift from hunter-gatherer egalitarian societies to a system based on rank lineages and inherited status, and (3) changing settlement patterns, such as the shift from circular shell rings to larger shell middens and mounds during later periods of time. In addition to its archaeological significance, Sapelo Island, and other islands along the Georgia coast, were and continue to be of special cultural significance to Native Americans, such as the Muscogee Nation. The Georgia barrier islands, as well as the interior of Georgia, are the traditional homelands of the Muscogee and other contemporaneous Native nations and tribes whose ancestors lived on the land for thousands of years, from the Late Archaic and up until the time of European colonization when the islands were ceded in the 1757 Treaty of Savannah.

The Sapelo Shell Ring Complex is located on the northwestern side of Sapelo Island. This site along with research on nearby Ossabaw and St. Catherines islands and regional surveys, has given key insight into the formation and abandonment of villages during the Late Archaic (5000–3000 BP) [7,11,12]. The Sapelo Shell Ring Complex consists of three circular shell rings (Rings I, II, and III) of varying size. Ring I is the largest, consisting of some 5660 m^3 of shell and covering an area of 6000 m^2. Archaeologists working in the Southeastern United states have debated as to why coastal groups built circular shell rings, specifically. Coastal groups continued to construct large shell middens during later periods of time; however, the circular and arcuate shapes are distinctive and unique to the Late Archaic period [13]. Most of these debates center around whether or not the rings were settings of large ceremonial gatherings or places of residence [2,4,14,15]. However, oxygen isotope analyses (δ^{18}O) of mollusk shells and seasonal signatures in archaeofaunal remains from the Sapelo Shell Ring complex indicate that these locales were occupied year-round, with some periods of more intensive gatherings [16,17]. More recent research by Thompson [4], suggests that the Sapelo Shell Ring Complex was a village likely comprised of coresidential communities characterized by group cooperation and collective action, especially regarding the harvesting of estuarine resources for subsistence and ceremonial purposes [4]. Furthermore, Thompson [4:30] argues, these villages emerged not because of individuals vying for power and prestige, but rather through the collective agency of groups that worked together to manage dynamic ecosystems that are highly sensitive to human activity and environmental change. Regarding the shape of Late Archaic shell rings, Thompson (4) also argues that the circular shape promoted social equality by discouraging aggrandizing and individualizing behaviors because the production and consumption behaviors of each household was visible to all. The Sapelo shell rings, as with most Late Archaic shell rings along the Georgia and South Carolina coast, are situated in locations with easy access to estuaries and oyster reefs.

As described above, the emergence and abandonment of the Sapelo shell rings during the Late Archaic seem to be correlated with local environmental change and instability. Rather than viewing this through a lens of environmental determinism, we argue that these changes are an indicator of a resilient socio-ecological system that was able to adapt to changing environmental circumstances; this is evidenced by the continued occupation of Native American groups on the Georgia coast from the Late Archaic period and up until the time of European colonization [9,10]. However, exactly what kind of environmental shifts occurred, to what degree, and on what time scale early villagers that lived on Sapelo Island during the Late Archaic period experienced such shifts have remained elusive. Here, we combine Bayesian chronological modeling of radiocarbon dates with multiple datasets, including oyster morphometrics, stable oxygen isotopes of mollusks, and recent tree ring analyses, to understand the nature and timing of environmental change associated with the emergence and abandonment of circular villages on Sapelo Island, Georgia, during the Late Archaic. Our overarching

objectives are to: (a) establish a chronological relationship between the three shell rings using Bayesian statistical modeling, and (b) use multiple environmental proxies (e.g., changes in oyster size and oxygen isotope values) to document environmental shifts across time that may have led to socio-ecological changes, specifically the formation and eventual cessation of circular shell ring construction on the Georgia coast.

Materials and methods

Radiocarbon samples and mollusk shells were collected from multiple levels of each shell ring in the Sapelo Shell Ring Complex. All mollusk shells used in this study are curated at the University of Georgia's Laboratory of Archaeology. Methods for radiocarbon analysis, paleobiology, and shell geochemistry are discussed in more detail below. Permission for field research and to collect samples on Sapelo Island were obtained from the Georgia Department of Natural Resources. Additionally, we consulted with the Muscogee Nation regarding research questions, methods, and interpretations of data presented here.

Radiocarbon analysis

Establishing a chronological relationship between the three Sapelo shell rings is necessary to link the formation and abandonment of the rings to one another, as well as environmental shifts over time. To examine the chronological relationship of the three rings, we obtained 17 new AMS radiocarbon dates across multiple proveniences from Shell Rings I, II, and III, along with 8 legacy dates. At the request of our Tribal collaborators, we avoided contexts containing ancestral remains in our dating project. Most of our dates come from hickory nut (*Carya* spp.), Unidentified (UID) nut fragments, deer bone, pine (*Pinus* spp.), sooted sherds, and UID carbonized wood.

All Accelerator Mass Spectrometry (AMS) radiocarbon measurements were carried out at the Center for Applied Isotope Studies (CAIS) facility at the University of Georgia and followed procedures outlined by Cherkinsky et al. [18]. The charcoal samples were treated following the acid/alkali/acid (AAA) protocol involving three steps: (a) an acid treatment (1N HCl at 80˚C for 1 hour) to remove secondary carbonates and acid-soluble compounds; (b) an alkali (NaOH) treatment; and (c) a second acid treatment (HCl) to remove carbonates ($CaCO_3$) that may absorb atmospheric CO_2. Sample was thoroughly rinsed with deionized water between each step, and the pretreated sample was dried at 105ºC. The dried charcoal was combusted at 900ºC in evacuated/sealed Pyrex ampoule in the presence of CuO.

The deer bone samples were cleaned by wire brush and washed, using an ultrasonic bath. After cleaning, the dried bones were gently crushed to small fragments. The cleaned samples were then reacted under vacuum with 1N HCl to dissolve the bone mineral and release carbon dioxide from bioapatite. The residues were filtered, rinsed with deionized water and under slightly acid condition (pH = 3) heated at 80ºC for 6 hours to dissolve collagen and leave humic substances in the precipitate. The collagen solution was then filtered to isolate pure collagen and dried out. The dried collagens were combusted at 575ºC in evacuated/sealed Pyrex ampoule in the presence CuO.

The resulting carbon dioxide was cryogenically purified from the other reaction products and catalytically converted to graphite as described in Cherkinsky et al. [15]. Graphite $^{14}C/^{13}C$ ratios were measured using the CAIS 0.5 MeV accelerator mass spectrometer. The sample ratios were compared to the ratio measured from the Oxalic Acid I standard (NBS SRM 4990). The sample $^{13}C/^{12}C$ ratios were measured separately using a stable isotope ratio mass spectrometer and expressed as $d^{13}C$ with respect to PDB, with an error of less than 0.1‰. The quoted uncalibrated dates have been given in radiocarbon years before 1950 (years BP), using

the ^{14}C half-life of 5568 years. The error is quoted as one standard deviation and reflects both statistical and experimental errors. The date has been corrected for isotope fractionation.

Oyster paleobiology

Eastern oysters (*Crassostrea virginica*), hereby simply referred to as oyster(s), were an important part of larger economic resources on the Georgia coast, and recent research shows that they were sustainably harvested by Native American communities for thousands of years [19,20]. Oysters were integral to other aspects of life as well, including their use in mound construction and shell ring formation, which can be seen at the Sapelo Shell Rings and later platform mounds along the Georgia coast, such as the Mississippian Period (1150–370 cal. BP) Irene Mound [21]. The size of oyster shells is determined by several factors including age, human predation pressures, and environmental variability, with healthier reefs and climatic stability generally producing larger oyster shells [22,23]. For these reasons, temporal changes in oyster size are used as a proxy for environmental change as well as human activity and harvesting practices [24,25].

To examine if there were any temporal changes in oyster size, we compared the size of eastern oysters between Sapelo Shell Ring I, II, and III. A total of 2,130 completely intact eastern oysters were measured from Sapelo Shell Rings I, II, and III. Left valve length (LVL) and left valve height (LVH) measurements (mm) were taken using digital, hand-held calipers, and following a standard method outlined in Lulewicz et al. [25]. All data analyses were conducted using the statistical software R. A Bartlett and Shapiro Wilk test were first used to examine homogeneity of variance and normality of the data, respectively. Since the data are not normally distributed or homoscedastic, a non-parametric Kruskal-Wallis test was used to compare mean LVH and LVL between shell rings, and a post-hoc pairwise Mann-Whitney U test was used to examine which rings are distinguishable regarding mean LVL and LVH. To reduce the possibility of type-I errors associated with multiple comparisons, a Holm correction was used with the Mann-Whitney U test.

Oyster geochemistry: Oxygen (δ^{18}O] isotope analysis

Oxygen Isotope (δ^{18}O) analysis of archaeological shell is a widely used method for reconstructing paleoclimate conditions, site occupation histories, and shellfish harvesting practices. Oxygen isotopic values in mollusk shells ($\delta^{18}O_{carbonate}$) are dictated by multiple variables, but largely are a function of the oxygen isotopes composition of ambient water ($\delta^{18}O_{water}$) [23–28]. Moreover, $\delta^{18}O_{water}$ covaries with salinity in coastal estuaries [29–32]. For these reasons, $\delta^{18}O_{carbonate}$ values in shell can be used to not only trace local environmental changes in the past, but also to explore Native American shellfish harvesting practices, such as season of collection and the range of habitats used for collection [33–42]. Here, we specifically use $\delta^{18}O_{carbonate}$ values to retrodict the salinity of the habitats where people harvested shell. As with shell size, changes in estimated salinity across time may point to changes in harvesting practices or environmental change. Scholars working in southeastern North America commonly use two species of mollusks in these studies: hard clams (*Mercenaria* spp.) and eastern oysters, which both have a wide salinity tolerance and are often found in close association. Hard clams tolerate salinity ranges between approximately 17 psu to 37+ psu, with optimal growth between 20 to 30 psu [43,44]. Oysters' salinity tolerance is slightly wider, from approximately 5 psu to 37+ psu, with optimal growth conditions between 14 and 28 psu [45,46].

Incremental oxygen (δ^{18}O) isotope analysis was conducted on both eastern oysters (n = 19) and hard clams (n = 59) collected from all three shell rings. Twenty of these shells were recently sampled; the rest are previously published data from Andrus and Thompson [33].

Laboratory protocols for $\delta^{18}O$ analysis were adapted from previous studies and are described elsewhere [18,33,39]. Briefly, only left oyster valves with a complete chondrophore and clam shells with an intact edge were selected for analysis. Shells with epibiont activity were excluded from analysis as they were likely dead when they were collected [47,48]. Next, oyster shells were bisected along the chondrophore and clams along their axis of maximum growth. The bisected shells were then mounted onto a slide using Crystalbond™ adhesive and cut into approximately 12.7-mm-thick sections using a slow-speed diamond wafering saw. Each shell was sampled following reverse ontogeny (starting at the ventral margin in clams and growing edge in oysters) using a Grizzly Benchtop micro-milling system. For oysters, sampling targeted internal chalky calcitic areas of each shell hinge and avoided the darker foliated calcite and aragonite regions closer to and on the hinge surface [28,49]. Sampling trajectories followed growth increments as seen in reflected light (in the chondrophore region of oysters and the middle shell layer in the clams) [18]. Oyster samples were taken adjacent to each other at an average of 300–400 mm in width and to a depth of 300–400 mm. For clams, samples were taken from the inner aragonite layers along the transected margin. Samples were taken sequentially starting at the ventral margin, and were milled to a depth of approximately 0.5-mm. Approximately, 12–20 samples were obtained from each oyster and 20 from each clam, which captured approximately one-year's worth of growth prior to collection.

The resultant powered carbonate samples were weighed using tin capsules and transferred into Exetainer® 12 ml borosilicate vials. All samples were analyzed for $\delta^{18}O$ and $\delta^{13}C$ using a Thermo Gas Bench coupled to a Delta V IRMS with a GC Pal auto-sampler at the University of Georgia's Center for Applied Isotope Analysis. The weighed samples were first purged of atmosphere with helium and acidified with phosphoric acid to convert solid carbonates to CO_2 gas. The target gas was then concentrated as a frozen solid within a loop submerged in a liquid nitrogen bath. After which, the gas was released back into the helium carrier gas to the IRMS. The values for each sample are reported in parts per mil (‰) relative to the VPDB standard by correcting to multiple NBS-19 analyses (typically 14) per run. NBS-19 was also used to assess and correct for drift and sample size linearity if needed.

Salinity was estimated from shell $\delta^{18}O$ values following published methods established for the local environments around Sapelo Island [18,50,51]. Eqs 1 and 2 were first used to estimate $\delta^{18}O_{water}$ values for each clam and oyster, respectively. The estimated $\delta^{18}O_{water}$ values were then used to predict salinity for each shell using Eq 3. Comparisons of estimated salinity were done between each shell ring for both species combined and each species separately.

Equations

$$\text{Water temperature}(^{\circ}C) = 20 - 4.42(\delta^{18}O_{argonite} - x) \tag{1}$$

whereas: 31°C is assumed to be the threshold of summer growth cessation for clams [31]; $\delta^{18}O_{argonite}$ is the most negative value in each clam's profile; and $x = \delta^{18}O_{water}$.

$$\text{Water temperature}(^{\circ}C) = 16.5 - 4.3(\delta^{18}O_{calcite} - x) + 0.14(\delta^{18}O_{calcite} - x)^2 \tag{2}$$

whereas: 28°C is assumed to be the threshold of summer growth cessation for oysters; $\delta^{18}O_{calcite}$ is the most negative value in each oyster's profile, and $x = \delta^{18}O_{water}$. Additionally, a 0.2‰ correction was applied to convert VPDB to VSMOW [50].

$$\delta^{18}O_{water} = 0.13(y) - 3.4 \tag{3}$$

whereas: $\delta^{18}O_{water}$ is calculated by Eqs 1 or 2, and y = estimated salinity (psu) [33].

Results

Radiocarbon models

Based on our knowledge of the types of samples, their overall contexts, and stratigraphic ordering, we constructed a series of Bayesian chronological models in OxCal 4.4.4. We then constructed an overall model to determine the ordering of the rings. The structure of the overall model follows closely to the models for each individual ring and can be seen in Fig 2A. We calibrated and modeled all dates using the IntCal20 curve [52], rounding to the nearest 5-year interval [53].

The results of our modeling of the dates indicate good agreement. Both the Amodel (79.2) and Aoverall (79.9) for the model indicate statistical significance, exceeding the 60-threshold established for Bayesian chronological analysis [53,54]. Due to the long tails in the distribution of these dates, here we focus on the 68% probability range; however, we also provide the 95% ranges (Table 1). All dates indicate good convergence (i.e., >95) save one date (UGAMS 15084), which appears to be anomalous and may be the result of bioturbation or some other factor. The model estimates a start date for Ring I of 4245–4175 cal. BP and an end date of 4150–4100 cal. BP; for Ring II, a modeled start date of 4290–4155 cal. BP and end date of 4085–3950 cal. BP; and for Ring III, a modeled start date of 4105–3985 cal. BP and end date of 3965–3845 cal. BP (Fig 2A).

To evaluate independently the sequence of occupation of the rings, we used the Order function in OxCal. This function provides probabilities for their relative order based on the dates for each ring. We then used R to calculate the posterior probability for various chronological relationships for the start and end date of the rings on Sapelo (Fig 2B). Based on these results, Ring II (4290–3950 cal. BP) appears to be the longest occupied seeing both the rise and abandonment of Ring I (4245–4100 cal. BP). The last generation to occupy Ring II likely also saw the founding of Ring III (ca 4105 cal. BP), which was likely founded after Ring I ceased to be used ca 4100 cal. BP.

Eastern oyster paleobiology

Our measurements show a clear distinction in oyster size between the three shell rings (Fig 3A, Table 2). Oyster shells from Ring I and Ring II are comparable in size and are generally larger than oysters from Ring III (Table 2). A non-parametric Kruskal-Wallis test indicates that the rings are significantly different regarding mean oyster height (LVH) and mean oyster length (LVL) (LVH: X^2 = 49.5, *p-value* < 0.01; LVL: X^2 = 39.8, *p-value* < 0.01). A post-hoc pairwise Mann-Whitney U test, however, shows that only oysters from Ring III are statistically smaller than Ring I and II regarding both LVH and LVL (at p-value < 0.01). Tests for equality of variance show a significant difference in variation among LVH and LVL between the shell rings, with Ring II exhibiting the greatest variation in oyster size (LVL: p < 0.001; LVH: p < 0.001).

Oyster geochemistry: Oxygen ($\delta^{18}O$) isotope analysis

Oxygen isotope results show a clear distinction between the shell rings regarding $\delta^{18}O_{carbonate}$, $\delta^{18}O_{water}$, and estimated salinity. Oxygen ($\delta^{18}O$) values varied among all oyster and clam shells: mean $\delta^{18}O_{carbonate}$ ranged between -4.0‰ to 0.5‰, and estimated $\delta^{18}O_{water}$ (using Eqs 1 and 2) ranged between -2.9‰ and 1.8‰ (Table 3). Most shells also show a general sinusoidal $\delta^{18}O_{carbonate}$ profile, indicating seasonal fluctuations in water temperature and allowing us to pinpoint summer $\delta^{18}O$ values (e.g., the most negative value within each shell profile) and predict salinity (Fig 4). Estimated salinity values ranged between 4 and 40 psu, indicating that inhabitants of all three rings were targeting a wide variety of habitats (Table 2). Most estimated
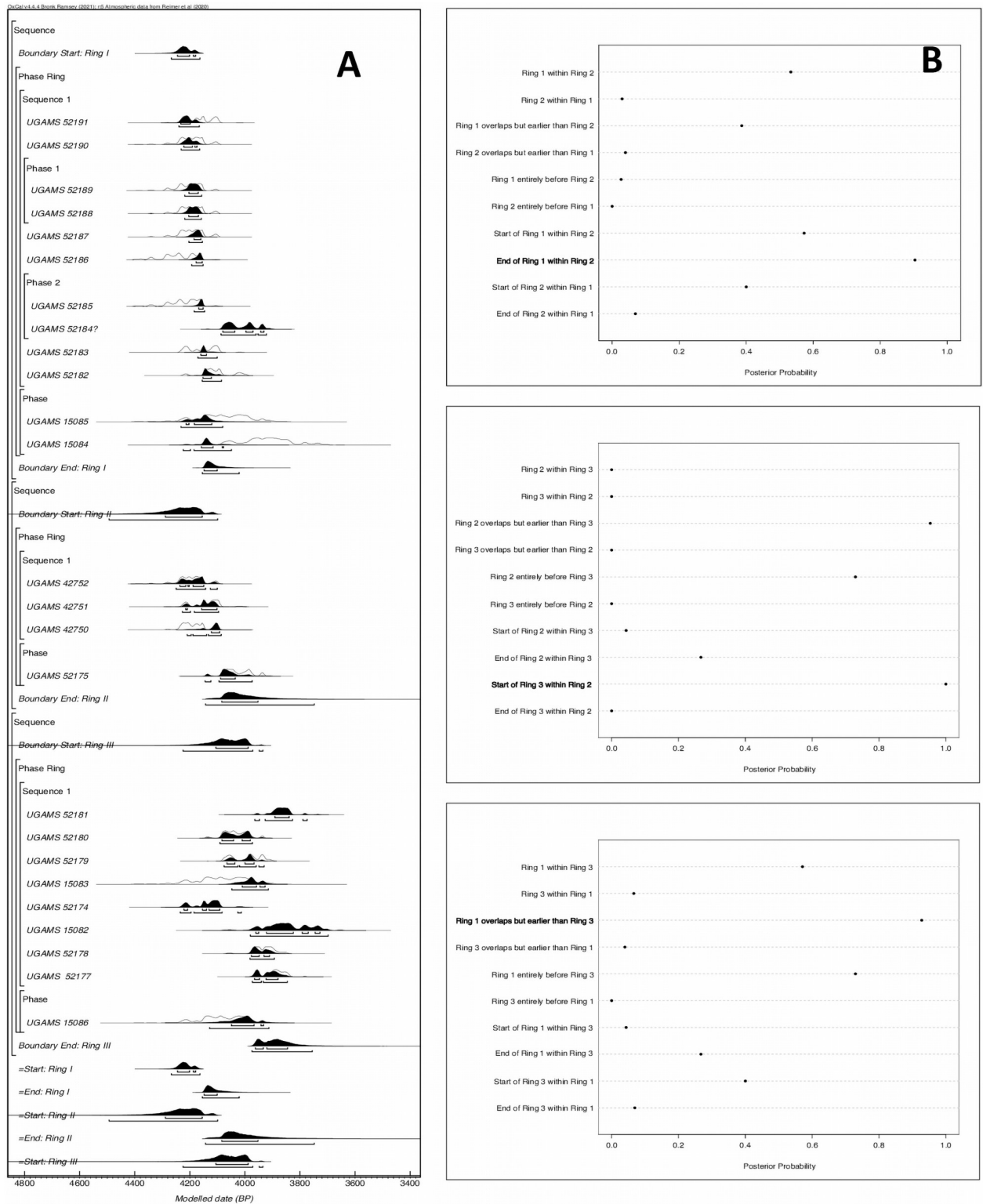
Fig 2. AMS models: (A) Probability distributions; (B) Posterior probability of the chronological relationships for the start and end date of the Sapelo shell rings.

https://doi.org/10.1371/journal.pone.0258979.g002

Table 1. Modeled dates from Sapelo Shell Rings I, II, and III.

Name	Unmodelled (BP)						Modelled (BP)						Amodel 104 Aoverall 101.3		
	from	to	%	from	to	%	from	to	%	from	to	%	Acomb	A	C
Sequence															
Boundary Start: Ring I							4245	4175	68.3	4270	4160	95.4			98.5
Phase Ring															
Sequence 1															
UGAMS 52191	4235	4095	68.3	4240	4090	95.4	4235	4195	68.3	4240	4165	95.4		107.7	99.3
UGAMS 52190	4240	4150	68.3	4290	4095	95.4	4225	4170	68.3	4235	4160	95.4		116.2	99.5
Phase 1															
UGAMS 52189	4245	4150	68.3	4295	4095	95.4	4205	4165	68.3	4220	4155	95.4		123.1	99.6
UGAMS 52188	4240	4150	68.3	4290	4095	95.4	4205	4165	68.3	4220	4155	95.4		117.2	99.6
UGAMS 52187	4240	4150	68.3	4290	4095	95.4	4185	4160	68.3	4205	4150	95.4		119.5	99.7
UGAMS 52186	4290	4155	68.3	4400	4150	95.4	4180	4155	68.3	4195	4150	95.4		112	99.9
Phase 2															
UGAMS 52185	4285	4150	68.3	4355	4145	95.4	4170	4150	68.3	4185	4145	95.4		111.9	99.9
UGAMS 52184	4080	3930	68.3	4090	3920	95.4	4080	3930	68.3	4090	3920	95.4			99.8
UGAMS 52183	4230	4090	68.3	4240	4085	95.4	4160	4135	68.3	4175	4100	95.4		103.5	99.9
UGAMS 52182	4155	4085	68.3	4225	3990	95.4	4155	4120	68.3	4155	4085	95.4		123.7	99.4
Phase															
UGAMS 15085	4220	3980	68.3	4290	3895	95.4	4215	4120	68.3	4235	4080	95.4		96.8	99.7
UGAMS 15084	4065	3835	68.3	4090	3720	95.4	4160	4075	68.3	4225	4045	95.4		17.4	99.4
Boundary End: Ring I							4150	4100	68.3	4155	4020	95.4			98.2
Sequence															
Boundary Start: Ring II							4290	4155	68.3	4495	4095	95.4			97.9
Phase Ring															
Sequence 1															
UGAMS 42752	4240	4150	68.3	4290	4095	95.4	4240	4145	68.3	4250	4100	95.4		102	99.4
UGAMS 42751	4225	4090	68.3	4235	4010	95.4	4215	4100	68.3	4230	4095	95.4		99.6	99.5
UGAMS 42750	4235	4145	68.3	4245	4090	95.4	4125	4090	68.3	4210	4085	95.4		70.9	99.9
Phase															
UGAMS 52175	4085	3975	68.3	4090	3925	95.4	4090	4035	68.3	4145	3970	95.4		99.7	99.5
Boundary End: Ring II							4085	3950	68.3	4145	3745	95.4			97.9
Sequence															
Boundary Start: Ring III							4105	3985	68.3	4225	3930	95.4			96.5
Phase Ring															
Sequence 1															
UGAMS 52181	3895	3835	68.3	3965	3770	95.4	3895	3835	68.3	3965	3770	95.4			99.6
UGAMS 52180	4085	3980	68.3	4140	3930	95.4	4085	3980	68.3	4095	3970	95.4		104.9	99.3
UGAMS 52179	4080	3925	68.3	4085	3900	95.4	4065	3965	68.3	4080	3930	95.4		101.7	99.7
UGAMS 15083	4220	3980	68.3	4290	3895	95.4	4010	3925	68.3	4050	3915	95.4		80.3	99.9
UGAMS 52174	4225	4090	68.3	4235	4010	95.4	4225	4090	68.3	4235	4010	95.4			99.6
UGAMS 15082	3960	3725	68.3	3980	3695	95.4	3960	3725	68.3	3980	3695	95.4			99.5
UGAMS 52178	3975	3895	68.3	3985	3845	95.4	3980	3910	68.3	3985	3890	95.4		109.4	99.9
UGAMS 52177	3960	3845	68.3	3975	3835	95.4	3965	3880	68.3	3975	3845	95.4		93.8	99.6
Phase															
UGAMS 15086	4150	3985	68.3	4240	3920	95.4	4050	3930	68.3	4130	3910	95.4		97.3	99.7
Boundary End: Ring III							3965	3845	68.3	3975	3755	95.4			97.4

(Continued)

Table 1. (Continued)

Name	Unmodelled (BP)						Modelled (BP)						Amodel 104 Aoverall 101.3		
	from	to	%	from	to	%	from	to	%	from	to	%	Acomb	A	C
Order															
Start: Ring I							4245	4175	68.3	4270	4160	95.4			98.5
End: Ring I							4150	4100	68.3	4155	4020	95.4			98.2
Start: Ring II							4290	4155	68.3	4495	4095	95.4			97.9
End: Ring II							4085	3950	68.3	4145	3745	95.4			97.9
Start: Ring III							4105	3985	68.3	4225	3930	95.4			96.5
End: Ring III							3965	3845	68.3	3975	3755	95.4			97.4

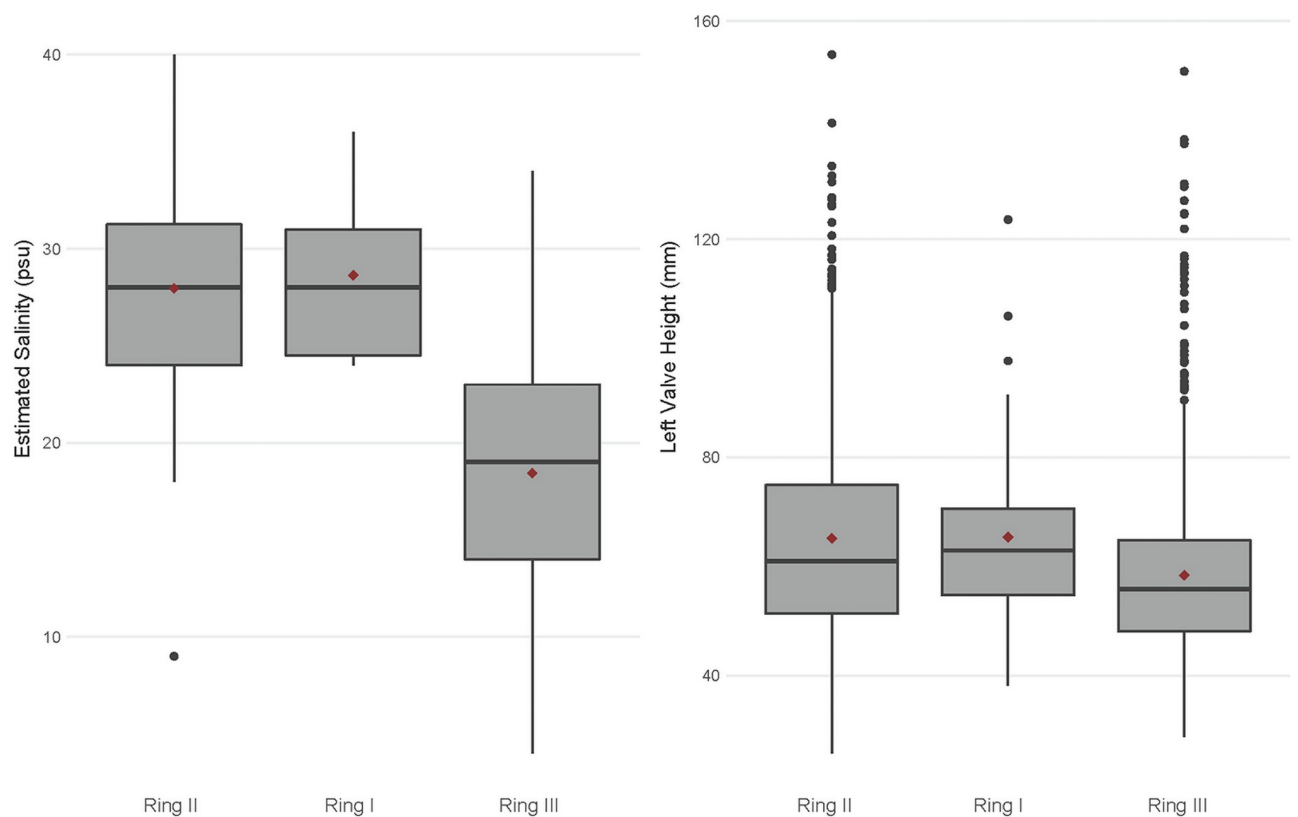https://doi.org/10.1371/journal.pone.0258979.t001

Fig 3. Box plots comparing (A) estimated salinity and (B) mean LVH between the three shell rings, showing significantly lower estimated salinity and smaller shells at Ring III. The shell rings are in chronological order based on the radiocarbon model, and red diamonds show mean values for each ring.

https://doi.org/10.1371/journal.pone.0258979.g003

Table 2. Descriptive statistics for oyster measurements and oxygen isotope analysis.

Shell Ring	N (Shell Measurements)	Mean LVL (mm)	Mean LVH (mm)	N (Shell Isotopes)	Mean $\delta^{18}O_{water}$	Mean Salinity (psu)
Ring I	65	35.3	65.3	11	0.2	28
Ring II	1057	34.1	65.3	46	0.2	28
Ring III	1008	32.1	58.4	21	-1.1	18

https://doi.org/10.1371/journal.pone.0258979.t002

Table 3. Estimated summer δ¹⁸O water (‰ VSMOW) values modeled after Andrus and Thompson's (2001) oxygen isotope-temperature equations (Eqs 1 and 2), assuming shell growth cessation at 28˚C for oysters and 31˚C for clams. Salinity (psu) calculated based on Eq 3.

Shell Ring	Species	Sample ID	$\delta^{18}O_{water}$ (‰)	Salinity (psu)
Shell Ring I	*Crassostrea virginica*	OLTS10	-0.2	25
Shell Ring I	*Crassostrea virginica*	OLTS9	-0.3	24
Shell Ring I	*Crassostrea virginica*	OLTS12	0.4	30
Shell Ring I	*Crassostrea virginica*	OLTS15	1.2	36
Shell Ring I	*Crassostrea virginica*	OLTS11	0.0	27
Shell Ring I	*Crassostrea virginica*	OLTS3	0.3	24
Shell Ring I	*Crassostrea virginica*	OLTS14	1.2	36
Shell Ring I	*Mercenaria* spp.	CLTS7	-0.9	29
Shell Ring I	*Mercenaria* spp.	CLTS6	0.2	28
Shell Ring I	*Mercenaria* spp.	CLTS4	-0.3	24
Shell Ring I	*Mercenaria* spp.	CLTS2	0.7	32
Shell Ring II	*Mercenaria* spp.	9MC23A-1-3SQ1S1	1.0	34
Shell Ring II	*Mercenaria* spp.	9MC23A-1-3SQ1S2	0.7	32
Shell Ring II	*Mercenaria* spp.	9MC23A-1-4SQ1S7	0.8	33
Shell Ring II	*Mercenaria* spp.	9MC23A-1-3SQ1S6	1.8	40
Shell Ring II	*Crassostrea virginica*	9MC23A-1-4SQ1S1	0.0	26
Shell Ring II	*Mercenaria* spp.	9MC23A-1-5SQ1S1	0.6	31
Shell Ring II	*Mercenaria* spp.	9MC23A-1-3SQ1S5	0.9	34
Shell Ring II	*Mercenaria* spp.	9MC23A-1-2SQ1S1	1.1	35
Shell Ring II	*Mercenaria* spp.	9MC23A-1-2SQ1S4	1.5	38
Shell Ring II	*Mercenaria* spp.	9MC23A-1-2SQ1S7	0.5	30
Shell Ring II	*Mercenaria* spp.	9MC23A-1-3SQ1S3	0.6	31
Shell Ring II	*Mercenaria* spp.	9MC23A-1-3SQ1S4	-2.2	9
Shell Ring II	*Mercenaria* spp.	9MC23A-1-3SQ1S7	0.7	32
Shell Ring II	*Mercenaria* spp.	9MC23A-1-2SQ1S5	0.9	34
Shell Ring II	*Mercenaria* spp.	9MC23A-1-2SQ1S3	1.5	38
Shell Ring II	*Mercenaria* spp.	9MC23A-1-2SQ1S2	0.9	34
Shell Ring II	*Crassostrea virginica*	9MC23A-1-4SQ1S4	-0.3	24
Shell Ring II	*Mercenaria* spp.	9MC23A-1-5SQ1S6	0.5	30
Shell Ring II	*Mercenaria* spp.	9MC23A-1-5SQ1S4	1.8	40
Shell Ring II	*Mercenaria* spp.	9MC23A-1-5SQ1S5	1.3	36
Shell Ring II	*Mercenaria* spp.	C5A	-0.3	24
Shell Ring II	*Mercenaria* spp.	C6A	-1.1	18
Shell Ring II	*Mercenaria* spp.	C6A	-0.9	19
Shell Ring II	*Mercenaria* spp.	C1A	-0.3	24
Shell Ring II	*Mercenaria* spp.	C25A	0.0	27
Shell Ring II	*Mercenaria* spp.	C2A	0.3	29
Shell Ring II	*Mercenaria* spp.	C3A	-0.3	24
Shell Ring II	*Mercenaria* spp.	C12A	-0.3	24
Shell Ring II	*Mercenaria* spp.	C7A	-0.2	25
Shell Ring II	*Mercenaria* spp.	C17A	-0.5	22
Shell Ring II	*Mercenaria* spp.	C9A	-0.1	26
Shell Ring II	*Mercenaria* spp.	C4A	-0.4	24
Shell Ring II	*Mercenaria* spp.	C11A	-0.5	23
Shell Ring II	*Mercenaria* spp.	C20A	-0.8	20
Shell Ring II	*Mercenaria* spp.	C24A	0.0	27

(*Continued*)

Table 3. (Continued)

Shell Ring	Species	Sample ID	$\delta^{18}O_{water}$ (‰)	Salinity (psu)
Shell Ring II	*Mercenaria* spp.	C18A	-0.2	25
Shell Ring II	*Mercenaria* spp.	C22A	0.0	26
Shell Ring II	*Mercenaria* spp.	C14A	0.1	27
Shell Ring II	*Mercenaria* spp.	C26A	0.2	28
Shell Ring II	*Mercenaria* spp.	C16A	0.1	27
Shell Ring II	*Mercenaria* spp.	C23A	0.5	31
Shell Ring II	*Mercenaria* spp.	C21A	0.2	28
Shell Ring II	*Mercenaria* spp.	C10A	0.3	29
Shell Ring II	*Mercenaria* spp.	C19A	0.3	29
Shell Ring II	*Mercenaria* spp.	C8A	0.5	30
Shell Ring II	*Mercenaria* spp.	C15A	0.4	29
Shell Ring III	*Crassostrea virginica*	O7	-2.9	4
Shell Ring III	*Crassostrea virginica*	O15	-1.5	15
Shell Ring III	*Crassostrea virginica*	O13	-1.9	12
Shell Ring III	*Crassostrea virginica*	O14	-0.8	20
Shell Ring III	*Crassostrea virginica*	O10	-0.4	23
Shell Ring III	*Crassostrea virginica*	O4	-0.4	23
Shell Ring III	*Crassostrea virginica*	O9	-1.1	18
Shell Ring III	*Crassostrea virginica*	O8	-0.5	23
Shell Ring III	*Crassostrea virginica*	O5	-0.3	24
Shell Ring III	*Crassostrea virginica*	O3	-0.9	34
Shell Ring III	*Mercenaria* spp.	C8	-2.4	8
Shell Ring III	*Mercenaria* spp.	C1	-1.9	12
Shell Ring III	*Mercenaria* spp.	C9	-1.0	19
Shell Ring III	*Mercenaria* spp.	C4	-1.6	14
Shell Ring III	*Mercenaria* spp.	C3	-1.8	13
Shell Ring III	*Mercenaria* spp.	C5	-1.5	15
Shell Ring III	*Mercenaria* spp.	C7	-0.9	19
Shell Ring III	*Mercenaria* spp.	C11	-0.8	20
Shell Ring III	*Mercenaria* spp.	C10	-0.8	20
Shell Ring III	*Mercenaria* spp.	C13	-0.1	26
Shell Ring III	*Mercenaria* spp.	C2	-0.3	24

salinity values fell within the salinity tolerance for each species, with only three shells falling outside of the expected range. At the mean level, the shell rings are significantly different regarding both $\delta^{18}O_{water}$ and estimated salinity ($\delta^{18}O_{water}$: $X^2 = 27$, *p-value* < 0.01; salinity: $X^2 = 32$, *p-value* < 0.01). A post-hoc pairwise Mann-Whitney U test, however, indicates that Shell Ring I and II are statistically indistinguishable, and only Ring III is statistically different, with more negative $\delta^{18}O_{water}$ values and lower estimated salinity (at p-value < 0.01) (Fig 3B). Tests for equality of variance finds that there is no significant difference in variation among $\delta^{18}O_{water}$ and estimated salinity for each shell ring ($\delta^{18}O_{water}$: *p-value* < 0.87; salinity: *p-value* < 0.37). These tests remained statistically significant when comparing oysters and clams separately.

Discussion

This research provides some of the most comprehensive evidence for environmentally correlated societal transformations on the Georgia coast during the Late Archaic, specifically
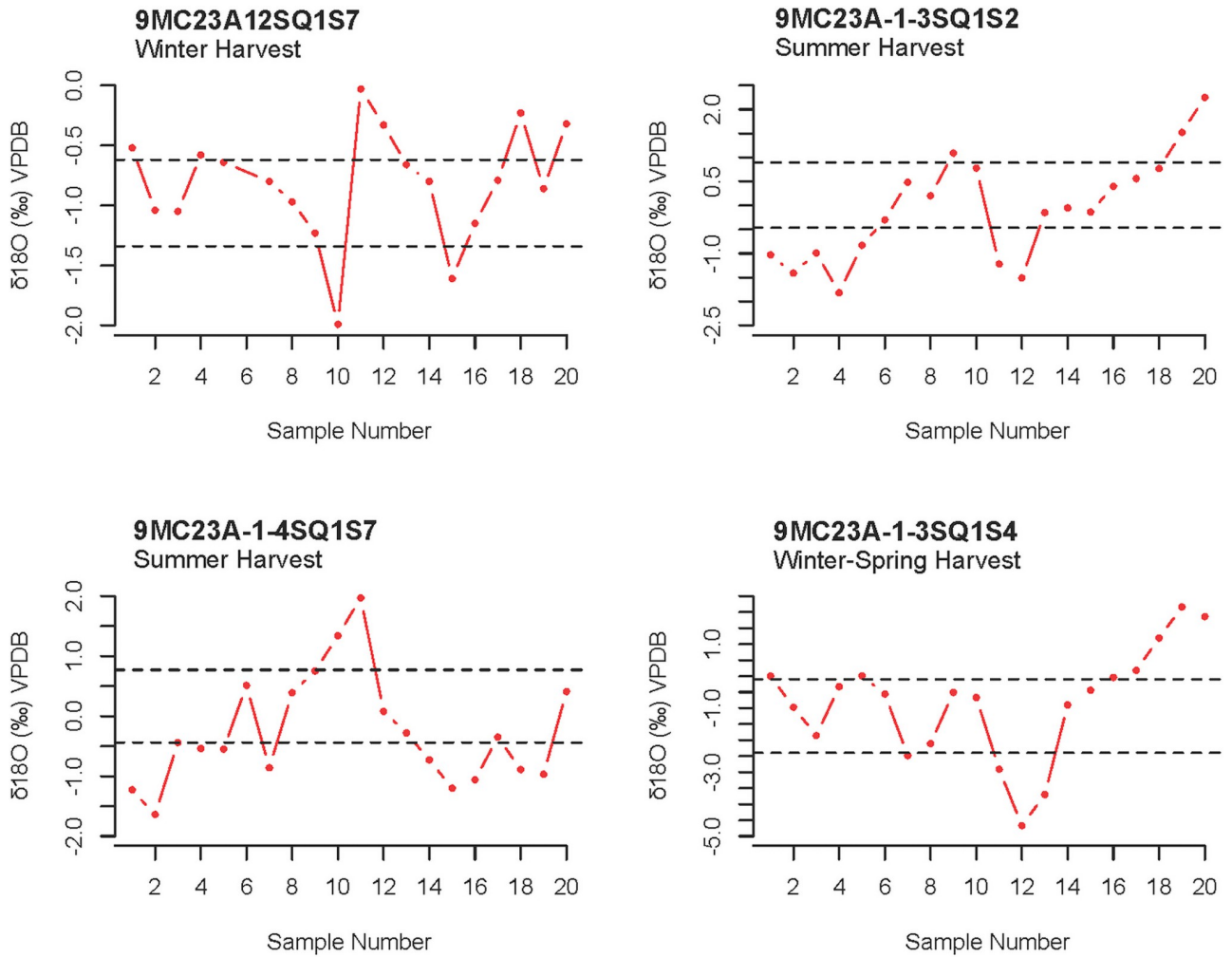
Fig 4. Examples of individual shell δ¹⁸O_carbonate profiles showing seasonal fluctuations in oxygen values and estimated season of harvest. The data sequence follows ontogeny from right to left, with the first value representing time of capture. The dashed lines in each graph represent the values that divide the sample range for each profile into equal thirds. If the first sample value falls below the bottom line the shell was collected in the summer, and if it falls above the top line then the shell was harvested in the summer. If the first value falls between the lines, then the shell was harvested in either the fall or spring.

https://doi.org/10.1371/journal.pone.0258979.g004
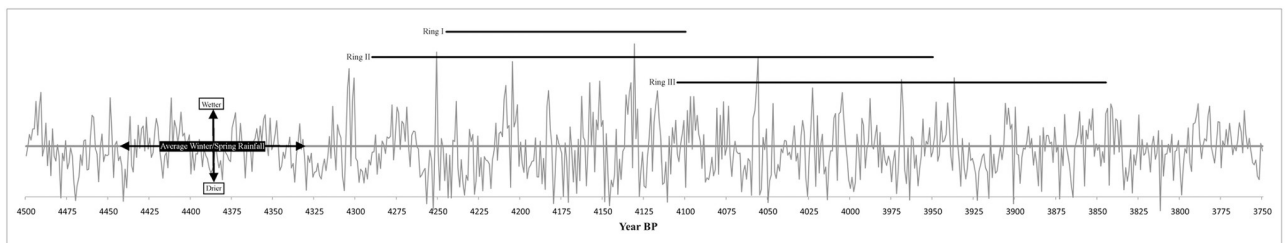
Fig 5. Temporally relevant portion of the multimillennial tree-ring chronology derived from a deposit of ancient buried bald cypress trees at the mouth of the Altamaha River. The chronology is in indices (standardized units representing average ring width, largely indicative in this locale of winter-spring precipitation), with "1000" indicating an annual ring of average width. Enhanced interannual rainfall variability and numerous very dry years are evident beginning around the earliest occupation of Ring I.

https://doi.org/10.1371/journal.pone.0258979.g005

regarding the formation and abandonment of circular shell villages on Sapelo Island. Our new chronological research indicates that Native Americans occupied the Sapelo shell rings at varying times with some generational overlap. Ring II had the longest occupational history, spanning from 4290 to 3950 cal. BP. Ring II also witnessed the emergence and abandonment of Ring I (4245 to 4100 cal. BP), as well as the rise of Ring III ca. 4105 cal. BP. By the end of the complex's occupation, only Ring III was occupied before its eventual abandonment around 3845 cal. BP.

Comparisons regarding oyster paleobiology and isotope geochemistry indicate that villagers at the shell ring complex experienced significant shifts in the environment, especially during the time in which Ring III was occupied. Ring III consists of significantly smaller oyster shells compared to Ring I and II. This suggests a temporal decrease in oyster size given that Ring III is the youngest of the three shell rings. Furthermore, even though Rings I and II had similar sized oyster shells that are significantly larger than those from Ring III, Ring II exhibits the greatest variation in oyster shell size, overlapping the range in shell size at the other two rings. This is likely attributed to the long occupational history of Ring II, which temporally overlaps with both Ring I and III. There are two ways to interpret the temporal trend in oyster size, though these drivers are not mutually exclusive and may be attributed to both. First, it is possible that oyster populations experienced harvesting pressures that resulted in smaller shells across time. For example, in heavily predated oyster populations, few individuals will make it to old age due to rapid turnover rates [55]. This results in oyster populations characterized by younger and smaller individuals. Environmental instability that affected local ecosystem productivity also may explain the decrease in oyster size across time. Lower salinity environments from reduced sea levels and periodic river flooding from a wetter climate have been shown to lead to high oyster mortality, regular intervals of growth cessation, and thus reduced oyster size [56–58]. Moreover, population densities and sedimentation rates can also impact oyster shape, with high population densities and sedimentation rates generally leading to elongated oyster shells, which helps the oyster reach sufficient nutrients [25,45]. Without other environmental proxies, however, it can be difficult to tease apart whether the observed patterns in oyster paleobiology were attributed to environmental change or human activity.

Results from our isotope geochemistry comparisons further support an interpretation that environmental instability was impacting local ecosystems during the Late Archaic. Oxygen isotope values in mollusk shells point to a shift toward lower salinity values in the estuaries in which mollusks were harvested, specifically during the time in which Ring III was occupied. This temporal pattern can be attributed to several factors, including previously documented changes in sea levels and local rainfall amounts, which both can impact the amount of fresh water input into local estuaries [5,6]. It is also possible that villagers who lived at Ring III were targeting mollusks further up estuaries, which are characterized by more freshwater input and thus lower salinity values. However, variation in estimated salinity values indicate that villagers at all three rings were targeting a wide range of habitats. This is corroborated by previously published data on vertebrate remains from Ring III (see supplemental information), which consists of marine fishes from a variety of habitats that could be captured year-round and using a range of fishing technologies [16]. Moreover, recent research shows that Native American communities along the South Atlantic coast sustainably harvested oysters for thousands of years, evidenced by an increase in oyster size from the Late Archaic through Mississippian periods (5000–370 cal. BP) [20]. This stands in contrast to an argument that changes in oyster sizes may reflect unsustainable human management practices. Taking all the evidence into consideration, it is likely that the observed patterns in oyster paleobiology and isotope geochemistry presented here were correlated with environmental fluctuations occurring on decadal or generational time scales.

Contextualizing the observed patterns in oyster paleobiology and isotope geochemistry with new environmental data derived from tree ring analysis in the locale, as well as our new radiocarbon model, provides a picture of how these early villagers negotiated environmental change that would have ultimately been observable across decades and generations. Recent dendrochronological data indicate a period of environmental instability, including high inter-annual variability in rainfall patterns, between 4300 and 3800 BP, which began to ameliorate post-3800 BP (Fig 5) [59]. These data contrast with previous research suggesting that environmental instability began around 3800 BP, around the time when people abandoned shell ring villages along the South Atlantic coast. Furthermore, this period of instability overlaps with the chronology of the entire Sapelo Shell Ring Complex, and further contextualizes the changes in oyster paleobiology and estimated salinity of targeted estuaries. Ring I was constructed and occupied during a period of high interannual variability in rainfalls as well as a rapid salinity intrusion event that kills multiple cypress trees, which likely contributed to higher estimated salinity values from oysters at both Rings I and II. Moreover, the time during which Ring III was occupied was overall wetter and had fewer very dry years compared to earlier occupations. A wetter environment leading to more fresh water input into local estuaries, in addition to relative sea level change, both explain the lower estimated salinity seen in oyster shells from Ring III.

These new data shift our focus from not just the abandonment of shell ring villages but also their emergence as an example of resilience in the face of environmental instability, such as changing rainfall patterns and sea levels that impacted resource availability. Thompson (2) argues that co-residential aggregation and collective action at the Sapelo shell ring villages would have provided a way to effectively manage oyster and other fisheries that are highly sensitive to environmental change and human activity. Our findings corroborate this argument by providing evidence of environmental instability experienced by successive generation of villagers on Sapelo Island, leading to societal transformations. As the local environment became unstable ca. 4300 BP, Native American communities on Sapelo Island underwent reorganization in both settlement and economies to navigate the shifting environmental conditions. More specifically, through aggregation, cooperation, and collective agency, these communities negotiated changing landscapes in the face of environmental instability documented here, specifically regarding the management of local fisheries. Given the chronological overlap of the shell rings, knowledge of how to sustainably manage fisheries would have been passed down across generations. Zooarchaeological data from Ring III, as well as the variability in oyster size and estimated salinity values shown here, suggest a persistence of subsistence and fishing strategies characterized by flexibility and use of an array of habitats—a necessity given the daily, seasonal, as well as decadal and generational environmental variability experienced by villagers on Sapelo Island. With continued environmental instability and sea level changes between 4200–3800 BP, the construction of shell ring villages ceased, and oyster fisheries on Sapelo Island collapsed ca. 3800 BP. However, environmental change is multidimensional; even as sea levels continued to drop, fluctuations between wet and dry periods began to stabilized post-3800 BP. People in the area adapted to these changes by shifting to a reliance on non-marine resources and new settlement patterns for a time (10).

We see similar patterns regarding the emergence and abandonment of other shell ring villages along the Georgia and South Carolina coast, with most ceasing during the Terminal Late Archaic period [9,11,60]. A few studies support an interpretation that other shell ring villages in the region also were abandoned in the face of environmental change. In addition to studies on sea level change, Lulewicz et al. [25] and Thompson et al. [20] show smaller oyster shells in the youngest deposits (dating towards the end of the Late Archaic Period) at Ossabaw, McQueen and St. Catherine shell rings, all located on the Georgia coast. However, the present

research is the first in the region to combine multiple environmental proxies with fine-scaled radiocarbon chronological modeling to examine correlations between the timing and nature of environmental instability and socio-ecological transformations. More research is needed to examine if these correlations exist at other Late Archaic circular shell rings along the Georgia and South Carolina coasts.

The emergence of village life and adaptation to coastal environments are key transitions in human history that occurred multiple times in a variety of geographic settings. As been the case in other areas of the word (e.g., Peru) where archaeologists intensely study these phenomena, the process by which people became embedded in these landscapes varied widely. Similar to other regions, the Native Americans that established North America's first villages also developed a complexity of ways to adapt to environmental fluctuations and resource shortfalls. This study provides high resolution climate and cultural datasets by which we examine how people reacted to and experienced climate change on a generational level. Climate change is complex and multidimensional as is how people adapt to and mediate their risk in such situations. Our example shows that the emergence of village life among Native Americas created novel social and economic circumstances that revolved around certain estuarine resources (e.g., mollusks). As succeeding generations that occupied the site began to experience environmental unpredictability and shifts in resources, occupants decided to alter these patterns to other locations and possible other kinds of social relationships. What is important in this case study is that even though these groups were generationally invested in a specific geographic place, they effectively adapted to changing circumstances and continue to occupy these coastal regions for millennia, albeit in different ways that built on the experience of generations past. This is perhaps a valuable lesson as a host of our current coastal cities and landmarks experience shifting climate and seas.

Supporting information

S1 Table. Sapelo Shell Ring Complex, Ring III, Unit 9 species list.
(DOCX)

S2 Table. Sapelo Shell Ring Complex, Ring III, Unit 4 species list.
(DOCX)

S3 Table. Uncorrected AMS dates and context for each sample. See Table 1 for corrected and modeled dates.
(DOCX)

S1 Text.
(DOCX)

S1 File. Oxcal code.
(DOCX)

Acknowledgments

Author Contributions

References

1. Birch J, Thompson, VD (eds) (2018) The archaeology of villages in eastern North America (University Press of Florida, Gainesville).

2. Sanger MC, Ogden QM (2018) Determining the use of Late Archaic shell rings using lithic data: "Ceremonial villages" and the importance of stone. *Southeastern Archaeology* 37(3):232–252.

3. Thomas DH (2008) Native American Landscapes of St Catherine's Island, Georgia. Anthropological Papers of the American Museum of Natural History, vol. 88, New York).

4. Thompson VD (2018). Collective Action and Village Life during the Late Archaic on the Georgia Coast. In: The archaeology of villages in eastern North America, eds Birch J, Thompson VD (University Press of Florida, Gainesville), pp 20–35.

5. Gayes PT, Scott DB, Collins ES, Nelson DD (1992) A Late Holocene sea-level fluctuation in South Carolina. In: Quaternary Coasts of the United States: Marine and Lacustrine Systems, eds Fletcher CH, Wehmiller JF (SEPM Society for Sedimentary Geology, Special Publication No. 48, Tulsa), pp 155–160.

6. Turck JA, Alexander CR (2013) Coastal landscapes and their relationship to human settlement on the Georgia coast. New York. In: Life Among the Tides: Recent Archaeology of the Georgia Bight, eds Thompson VD, Thomas DH (Anthropological Papers of the American Museum of Natural History, vol. 98, New York), pp 169–189.

7. Sanger MC (2010) Leaving the rings: shell ring abandonment and the end of the Late Archaic. In: Trend, Tradition, and Turmoil: what Happened to the Southeastern Archaic? eds Thomas DH, Sanger MC (American Museum of Natural History Anthropological Papers, No. 93, New York), pp. 201–216.

8. Thompson VD, Turck JA (2009) Adaptive cycles of coastal hunter-gatherers. *American Antiquity* 74(2):255–278.

9. Turck JA, Thompson VD (2016) Revisiting the resilience of late archaic hunter-gatherers along the Georgia coast. *Journal of Anthropological Archaeology* 43:39–55.

10. Ritchison BT, Thompson VD, Lulewicz I, Tucker B, Turck JA (2021) Climate change, resilience, and the Native American Fisher-hunter-gatherers of the late Holocene on the Georgia coast, USA. *Quaternary International* 584:82–92.

11. Thomas DH, Sanger MC (2010) The two rings of St. Catherines Island: Some preliminary results from the St. Catherines and McQueen shell rings. In: Trend, Tradition, and Turmoil: what Happened to the Southeastern Archaic? eds Thomas DH, Sanger MC (American Museum of Natural History Anthropological Papers, No. 93, New York), pp. 45–70.

12. Thompson VD, Turck JA (2010) Island archaeology and the Native American economies (2500 B.C. to A.D. 1700) of the Georgia Coast, USA. *Journal of Field Archaeoleology* 35:283–297.

13. Russo M (2014) Ringed Shell Features of the Southeastern United States. In: *The Cultural Dynamics of Shell-matrix Sites*, eds. Roksandic Mirjana, de Souza Sheila Mendonça, Eggers Sabine, Burchell Meghan, and Klokler Daniela (University of New Mexico Press, Albuquerque), pp. 21–39.

14. Rebecca S (2014) Shell Rings of the Lower Atlantic Coast of the United States In: The Cultural Dynamics of Shell-matrix Sites, eds. Roksandic Mirjana, de Souza Sheila Mendonça, Eggers Sabine, Burchell Meghan, and Klokler Daniela (University of New Mexico Press, Albuquerque), pp. 41–55.

15. DePratter CB (1976). *Shell mound Archaic on the Georgia coast* (Vol. 8). Archeological Society of South Carolina.

16. Colaninno CE, Compton JM (2019) Integrating vertebrate and invertebrate seasonality data from Ring III of the Sapelo Island Shell Ring Complex (9MC23). *Journal of Island and Coastal Archaeology* 14 (4):560–583.

17. Thompson VD, Andrus CFT (2011) Evaluating mobility, monumentality, and feasting at the Sapelo Shell Ring complex. *American Antiquity* 76:315–344.

18. Cherkinsky A, Culp RA, Dvoracek DK, Noakes JE (2010) Status of the AMS facility at the University of Georgia. *Nuclear Instruments and Methods in Physics Research* 268:867–870.

19. Reede-Myers LA, Thompson VD, Rick TC, et al. (Under Review). Forgotten Fisheries, Indigenous Communities, and the Shifting Baseline of Global Oyster Harvest. *Submitted to Nature Sustainability*.

20. Thompson VD, Rick T, Garland CJ, Thomas DH, Smith KY, Bergh, et al. (2020) Ecosystem stability and Native American oyster harvesting along the Atlantic Coast of the United States. *Science Advances* 6(28):1–8 9652. https://doi.org/10.1126/sciadv.aba9652 PMID: 32832610

21. Thompson VD (2009) The Mississippian production of space through earthen pyramids and public buildings on the Georgia coast, USA. *World Archaeology* 41(3):445–470.

22. Bartol IK, Mann R, Luckenbach M (1999) Growth and mortality of oysters (*Crassostrea virginica*) on constructed intertidal reefs: effects of tidal height and substrate level. *Journal of Experimental Marine Biology and Ecology* 237:157–184.

23. Claassen C (1998) *Shells*. (Cambridge University Press, Cambridge).

24. Morrison AE, Cochrane EE (2008) Investigating shellfish deposition and landscape history at the Natia Beach site, Fiji. *Journal of Archaeological Science* 35(8):2387–2399.

25. Lulewicz IH, Thompson VD, Cramb J, Tucker B (2017) Oyster paleoecology and native American subsistence practices on Ossabaw Island, Georgia, USA. *Journal of Archaeological Science*: *Reports* 15:282–289.

26. Jones DS, Arthur MA, Allard DJ (1989) Sclerochronological record of temperature and growth from shells of Mercenaria from Narragansett Bay, Rhode Island. *Marine Biology* 102:225–234.

27. Kirby MX, Soniat TM, Spero HJ (1998) Stable isotope sclerochronology of Pleistocene and recent oyster shells (*Crassostrea virginica*). *Palaios* 13:560–569.

28. Surge D, Lohmann C, Goodfriend GA (2003) Reconstructing estuarine conditions: oyster shells as recorders of environmental change, Southwest Florida. *Estuarine*, *Coastal*, *and Shelf Science* 57:737–756.

29. Elliot M, deMenocal PD, Linsley BK, Howe SS (2003) Environmental controls on the stable isotopic composition of Mercenaria: potential application to paleoenvironmental studies. *Geochemistry*, *Geophys*, *Geosys* 4:1–16.

30. Andrus CFT, Crowe DE (2000) Geochemical analysis of Crassostrea virginica as a method to determine season of capture. *Journal of Archaeological Science* 27:33–42.

31. Coplen TB, Kendall C (2000) Stable hydrogen and oxygen isotope ratios for selected sites of the U.S. geological survey's NASQAN and benchmark surface water networks. *U.S. Geol. Surv. Open-File Rept*. 0–160.

32. Andrus CFT (2011) Shell midden sclerochronology. *Quaternary Science Reviews* 30:2892–2905.

33. Andrus CFT, Thompson VD (2012) Determining the habitats of mollusk collection at the Sapelo Island shell ring complex, Georgia, USA using oxygen isotope sclerochronology. *Journal of Archaeological Science* 39:215–228.

34. Blitz JH, Andrus CFT, Downs LE (2014) Sclerochronological measures of seasonality at a Late Woodland mound on the Mississippi Gulf Coast. *American Antiquity* 79(4):697–711.

35. Burchell M, Cannon A, Hallmann, Schwarcz HP, Schöne BR (2013) Refining estimates for the season of shellfish collection on the Pacific Northwest coast: Applying high-resolution stable oxygen isotope analysis and schlerochronology. *Archaeometry* 55(2):258–276.

36. Hausmann N, Meredith-Williams M (2016) Seasonal patterns of coastal exploitation on the Farasan Islands, Saudi Arabia. *Journal of Island and Coastal Archaeology* 00:1–20.

37. Lesure RG, Gagiu A, Culleton BJ, Kennett DJ (2009) Changing patterns of shellfish exploitation at El Varal. In: Settlement and Subsistence in Early Formative Sonconusco: El Varal and the Problem of Inter-Site Assemblage Variation, ed Lesure RG (Cotsen Institute of Archaeology, pp. 75–87.

38. Lulewicz IH, Thompson VD, Pluckhahn TJ, Andrus CFT, Das O (2018) Exploring oyster (*Crassostrea virginica*) habitat collection via oxygen isotope geochemistry and its implications for ritual and mound construction at Crystal River and Roberts Island, Florida. *The Journal of Island and Coastal Archaeology* 13(3):388–404.

39. Lulewicz IH, Wallis NJ, Thompson VD (2019) Exploring the season of mound building through oxygen isotope geochemistry at the Garden Patch site, Gulf Coast Florida, USA. *Southeastern Archaeology* 39 (1):16–28.

40. Thompson VD, Andrus CFT (2013) Using oxygen isotope sclerochronology to evaluate the role of small island among the Guale (AD 1325 to 1700) of the Georgia Coast, USA. *Journal of Island and Coastal Archaeology* 8(2):190–209.

41. Twaddle RW, Ulm S, Hinton J, Wurster CM, Bird MI (2015) Sclerochronological analysis of archaeological mollusk assemblages: Methods, applications, and future prospects. *Archaeological and Anthropological Sciences* 8(2):359–379.

42. Walker KJ, Surge D (2006) Developing oxygen isotope proxies from archaeological sources for the study of Late Holocene human climate interactions in coastal southwest Florida. *Quat. Int*. 150:3–11.

43. Kraeuter JN, Castagna M (2001) *Biology of the Hard Clam* (Elsevier Science, New York).

44. Grizzle RE, Bricelj VM, Shumway SE (2001) Physiological ecology of Mercenaria. In: Biology of the Hard Clam, eds Kraeuter JN, Castagna M (Elsevier Science, New York), pp. 305–382.

45. Bartol IK, Mann R, Luckenbach M (1999) Growth and Mortality of Oysters (Crassostrea virginica) on Constructed Intertidal Reefs: Effects of Tidal Height and Substrate Level. *Journal of Experimental Marine Biology and Ecology* 237:157–184.

46. Shumway SE (1996) Natural environmental factors. In: The Eastern Oyster Crassostrea virginica, eds Kennedy VS, Newell RIE, Eble AF (Maryland Sea Grant College, College Park), pp. 467–513.

47. Cobb WR (1969) Penetration of Calcium Carbonate Substrates by the Boring Sponge *Cliona*. *American Zoologist* 9:783–790.

48. Warburton FE (1958) The Manner in which the Sponge *Cliona* Bores in Calcareous Objects. *Canadian Journal of Zoology* 36:555–562.

49. Carriker MR, Palmer RE (1979) A new mineralized layer in the hinge of the oyster. *Science* 206 (4419):691–693. https://doi.org/10.1126/science.206.4419.691 PMID: 17796935

50. Harding JM, Spero HJ, Mann R, Herbert GS, Sliko JL, Kennett JP (2010) Reconstructing early 17th century estuarine drought conditions from Jamestown oysters. *Proc Natl Acad Sci USA* 107:10549–10554. https://doi.org/10.1073/pnas.1001052107 PMID: 20534581

51. Epstein S, Buchsbaum R, Lowenstam HA, Urey HC (1953) Revised carbonate-water isotopic temperature scale. *Geological Society of America Bulletin* 64(11):1315–1326.

52. Reimer PJ, Austin WE, Bard E, Bayliss A, Blackwell PG, Ramsey CB, et al (2020) The IntCal20 Northern Hemisphere radiocarbon age calibration curve (0–55 cal kBP). *Radiocarbon* 62(4):725–757.

53. Hamilton WD, Krus AM (2018) The myths and realities of Bayesian chronological modeling revealed. *American Antiquity* 83(2):187–203.

54. Bronk-Ramsey C (2009) Bayesian Analysis of Radiocarbon Dates. *Radiocarbon* 51(1):337–360.

55. Rick TC, Reeder-Myers LA, Hofman CA, Breitburg D, Lockwood R, et al. (2016) Millennial-scale sustainability of the Chesapeake Bay Native American oyster fishery. *Proc Natl Acad Sci USA* 113 (23):6568–6573. https://doi.org/10.1073/pnas.1600019113 PMID: 27217572

56. Wang H, Huang W, Harwell MA, Edmiston L, Johnson E, Hsieh P, et al (2008) Modeling oyster growth rate by coupling oyster population and hydrodynamic models for Apalachicola Bay, Florida, USA. *Ecological Modelling* 211(1–2):77–89.

57. La Peyre MK, Gossman B, La Peyre JF (2009) Defining optimal freshwater flow for oyster production: Effects of freshet rate and magnitude of change and duration on eastern oysters and Perkinsus marinus infection. *Estuaries and Coasts* 32(3):522–34.

58. La Peyre MK, Eberline BS, Soniat TM, La Peyre JF (2013) Differences in extreme low salinity timing and duration differentially affect eastern oyster (Crassostrea virginica) size class growth and mortality in Breton Sound, LA. *Estuarine, Coastal and Shelf Science* 135:146–57.

59. Napora KG (2020). Refining cultural and environmental temporalities at the Late Archaic—Early Woodland Transition on the Georgia Coast, USA. Ph.D. Dissertation, University of Georgia.

60. Sanger MC, Seeber K, Bourcy S, Galdun J, Troutman M, Mahar G, et al (2021) Revelatory locales: The ritual reuse of a Late Archaic shell ring in South Carolina. *Journal of Anthropological Archaeology* 64:101356.